Separation Science and Technology
Publication details, including instructions for authors and subscription information:
http://www.informaworld.com/smpp/title~content=t713708471

Fluid Mechanics-Foam Flotation Interactions

Richard M. French[a]; David J. Wilson[b]
[a] WATER RESOURCES CENTER DESERT RESEARCH INSTITUTE, LAS VEGAS, NEVADA [b] DepartmentS OF CHEMISTRY AND ENVIRONMENTAL ENGINEERING, VANDERBILT UNIVERSITY, NASHVILLE, TENNESSEE

To cite this Article French, Richard M. and Wilson, David J.(1980) 'Fluid Mechanics-Foam Flotation Interactions', Separation Science and Technology, 15: 5, 1213 — 1227
To link to this Article: DOI: 10.1080/01496398008066967
URL: http://dx.doi.org/10.1080/01496398008066967

SEPARATION SCIENCE AND TECHNOLOGY, 15(5), pp. 1213–1227, 1980

Fluid Mechanics–Foam Flotation Interactions

RICHARD M. FRENCH

WATER RESOURCES CENTER
DESERT RESEARCH INSTITUTE
LAS VEGAS, NEVADA 89109

DAVID J. WILSON

DEPARTMENTS OF CHEMISTRY AND ENVIRONMENTAL ENGINEERING
VANDERBILT UNIVERSITY
NASHVILLE, TENNESSEE 37235

Abstract

Foam flotation methods have been used for years for ore concentration and show considerable promise for the removal of a variety of pollutants from wastewaters. However, scant attention has been given to the critical interaction in these processes of surface chemistry and fluid mechanics. A numerical model of an air bubble with an attached floc particle rising in a Stokes flow regime through a liquid pool at the bottom of a batch foam flotation column was developed. This model computed the viscous forces acting to separate the bubble and particle, and these forces were compared with those given by previous investigators. This research demonstrates that, while previous methods have correctly estimated the magnitudes of the viscous forces, they have failed to correctly estimate the directions. Based on the results of this work, a much simpler model for describing the interaction of fluid mechanics and surface chemistry in particle attachment to bubbles in foam flotation columns is suggested.

INTRODUCTION

Although foam flotation methods have been used for years for ore concentration and show considerable promise for the removal of a variety of pollutants from wastewasters (*5*), scant attention has been shown to the critical interaction in these processes of surface chemistry and fluid mechanics. While the forces binding a floc particle to the surface of an air

bubble may be accurately estimated, the viscous forces tending to separate the particle and the bubble cannot, at present, be accurately estimated under all flow conditions.

The purpose of this research was to develop a mathematical model which could accurately estimate the viscous forces on a floc particle attached to an air bubble rising through a liquid pool at the bottom of a batch foam flotation column. The rise velocity of the bubble was assumed to be such that the Reynolds number was less than 1, and hence the bubble was in a creeping flow regime. The viscous forces acting to separate the bubble and particle computed in this research were compared with those previously estimated by Currin et al. (*2*), and it was demonstrated that although this method adequately estimated the magnitudes of these forces, it failed to correctly estimate the directions. The primary significance of this research is that it suggests new avenues of research and a much simpler model for describing the interaction of fluid mechanics and surface chemistry in particle attachment to bubbles in foam flotation columns.

ANALYSIS

The analysis of the fluid motion past an air bubble with an attached floc particle, Fig. 1, must begin with the Navier-Stokes equations of flow for a viscous, steady, incompressible fluid and the corresponding equation of continuity. At present, there appear to be no exact solutions to these equations for flow past bodies of finite size; consequently, it is necessary to derive approximate solutions. These approximate solutions may be

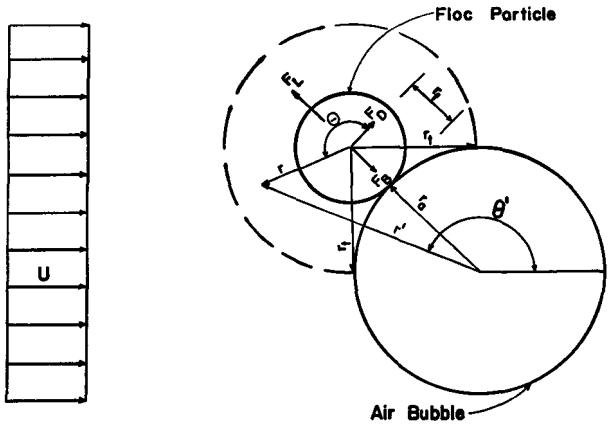

FIG. 1. Schematic definition of air bubble–floc particle system.

either numerical solutions of the exact Navier-Stokes equations or solutions, either numerical or analytical, of approximate equations. In either case, the dominant parameter involved is the Reynolds number, Re, and a value of this parameter must be specified. In the extreme case considered here, Re < 1, the Navier-Stokes equations reduce to the Stokes equations:

$$\text{grad}\, p = \mu \nabla^2 \mathbf{v} \tag{1}$$

and

$$\text{div}\, \mathbf{v} = 0 \tag{2}$$

(The symbols are defined at the end of the text.) Equations (1) and (2) are subject to the same boundary conditions as the complete Navier-Stokes equations, namely the no-slip boundary condition and no penetration of solid boundaries by fluid, i.e.,

$$v_n = 0 \tag{3}$$

and

$$v_t = 0 \tag{4}$$

In the case of low Reynolds number flow past a sphere, it is convenient to introduce spherical polar coordinates r, θ, and λ with the axis $\theta = 0°$ aligned in the direction of the free stream velocity U. Equation (2), the equation of continuity, is satisfied if the radial and theta velocity components, v_r and v_θ, respectively, are defined in terms of the Stokes stream function ψ, i.e.,

$$v_r = \frac{1}{r^2 \sin\theta} \frac{\partial \psi}{\partial \theta} \tag{5}$$

and

$$v_\theta = -\frac{1}{r \sin\theta} \frac{\partial \psi}{\partial r} \tag{6}$$

In the absence of swirl, $v_\lambda = 0$, substitution of Eqs. (4) and (5) in Eq. (1) yields

$$\left(\frac{\partial^2}{\partial r^2} + \frac{\sin\theta}{r^2} \frac{\partial}{\partial \theta} \left(\frac{1}{\sin\theta} \right) \frac{\partial}{\partial \theta} \right)^2 \psi = 0 \tag{7}$$

which is the equation of Stokes (*4*).

In Fig. 1 the air bubble–floc particle system is shown schematically; in contrast with the actual application of this research, the bubble–particle system is assumed stationary in a free stream velocity field of magnitude U.

With regard to this situation, several simplifying assumptions must be made. First, the analysis of the system described here begins at some time after the bubble and particle come into contact. The bubble and particle are assumed to be pinned together at the point of contact, and the magnitude of this binding force can be estimated by the methods of Wilson (*10*). The floc particle is thus subject to three forces; the binding force F_B, a drag force F_D, and a lift force F_L. These forces are defined in Fig. 1. Second, it is assumed that the mass and volume of the particle are negligible, and that the drag contributed by the particle to the bubble–particle system is negligible. Third, the air bubble and floc particle are idealized as perfect, solid spheres with radii r_a and r_f, respectively. Batchelor (*1*) has noted that gas bubbles may be expected to remain spherical if

$$\rho g^2 r_a^2 / v^2 \sigma \ll 81 \tag{8}$$

Forth the internal motion of the gas in the bubble is assumed to have no effect on the liquid motion. Fifth, the external pressure field is assumed to be constant. Sixth, the flow about the bubble–particle system is assumed to be axisymmetric, i.e., $v_\lambda = 0$. Although the flow is not truly axisymmetric, the magnitude of r_f relative to r_a is such that this is a reasonable simplification. Seventh, it is assumed that the bubble–particle system is in an infinite flow field, i.e., there are no walls to influence the flow.

Given these assumptions, it is convenient to establish a bipolar coordinate system and specify the boundary conditions and solution in terms of the polar coordinate system with its origin at the center of the floc particle, Fig. 1. It is also convenient to define a dimensionless stream function

$$\psi' = \psi / U r_a^2 \tag{9}$$

A uniform velocity or stream function field exists very far from the bubble–particle system. Far from the bubble-particle system, the flow appears as if only the air bubble were present. For both of these areas, the stream function is given by

$$\psi' = 0.5 \sin^2(\theta') \left(\frac{r'}{2r_a} - \frac{3r_a}{r'} + \frac{(r')^2}{r_a^2} \right) \tag{10}$$

which is the Stokes solution (*9*). By definition, the streamline which coincides with the air bubble–floc particle boundary is $\psi' = 0$. This definition implicitly satisfies the boundary condition given by Eq. (4). The boundary condition given by Eq. (3) requires that at the air bubble–floc particle boundaries

$$\partial \psi' / \partial n = 0 \tag{11}$$

where n = coordinate direction normal to the boundary. Equation (10) defines ψ' for

$$r \geq 0.75r_t \tag{12}$$

where r_t is a line constructed through the center of the floc particle tangent to the surface of the air bubble, Fig. 1. For r less than $0.75r_t$, ψ' must be computed from Eq. (7) where ψ' is substituted for ψ. It is noted that, once r_a and r_f are defined, r_t remains constant for all θ', since a sphere has constant curvature. Given Fig. 1, basic geometry and trigonometry are sufficient to locate all boundaries.

Given the foregoing boundary conditions, Eq. (7) can be solved numerically, and after converting the resulting ψ' values to values of ψ, v_r and v_θ can be found from Eqs. (5) and (6). It is noted that for $\theta = 180$ or $0°$, v_r and v_θ are not defined. The distribution of pressure throughout the fluid is determined by integrating Eq. (1), and the corresponding shear stress distribution is given by

$$\tau_{r\theta} = \mu\left(\frac{1}{r}\frac{\partial v_r}{\partial \theta} + \frac{\partial v_\theta}{\partial r}\right) \tag{13}$$

where $\tau_{r\theta}$ = shear stress acting in the θ direction on a plane whose normal is the r direction. The drag on the floc particle is then found by integrating the pressure and shear over the surface of the floc particle, i.e.,

$$F_D = -\int_0^\pi \tau_{r\theta|r=r_f} \sin\theta \, dA - \int_0^\pi p_{|r=r_f} \cos\theta \, dA \tag{14}$$

where F_D = drag force on the floc particle and $dA = 2\pi r_f^2 \sin\theta \, d\theta$. The lift is found in an analogous fashion:

$$F_L = -\int_0^\pi \tau_{r\theta|r=r_f} \cos\theta \, dA - \int_0^\pi p_{|r=r_f} \sin\theta \, dA \tag{15}$$

where F_L = life force on the floc particle and $dA = 2\pi r_f^2 \cos\theta \, d\theta$. The lift arises because the flow is not axisymmetric, and the lift is the only force considered in this analysis which would tend to separate the bubble and particle.

NUMERICAL CALCULATIONS

Given that Eq. (10) defines ψ' for all r greater than or equal to $0.75r_t$, Eq. (7) must then be solved for the remaining domain of (r, θ) subject to the noted boundary conditions. This remaining (r, θ) domain was covered with a circular grid having a distance Δr between the nodes in the r direction and $\Delta\theta$ in the theta direction. A rather standard finite

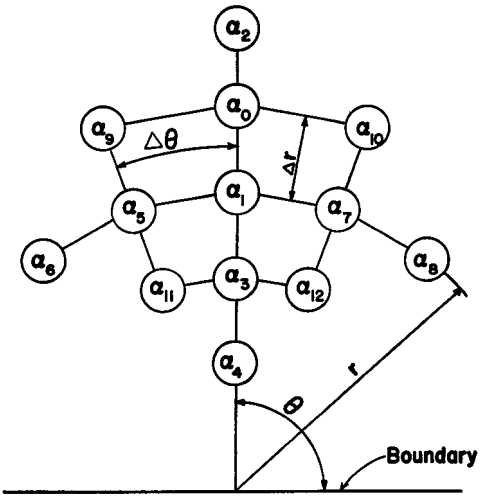

FIG. 2. Computational star for a typical interior mesh node.

difference scheme was then applied; e.g., Street (*8*). The computational star for the typical interior node is shown in Fig. 2, and the coefficients for this star are defined in the section entitled "Numerical Coefficients." From Fig. 2 it is noted that the numerical scheme is implicit, and therefore the numerical solution required that Eq. (7) be written at each node. The result was M simultaneous equations. In the case considered here, M was equal to 316 and a standard elimination scheme was used to solve the equations.

Vanderbilt University's DEC 1099 computer system was used for all computations. The size of the program developed required that the calculations be accomplished in three steps. An initial program, FL, solved Eq. (7) on the basis of a coarse radial grid, Table 1. FL generated a data file which was used as input to a second program, FLLOAD, which solved Eq. (7) on the basis of a much finer radial grid. The angular grid for FL and FLLOAD was constant. FLLOAD generated a data file which was

TABLE 1

Summary of Numerical Parameters

Parameter	FL	FLLOAD
r_t	4.6×10^{-6}	4.6×10^{-6}
Δr	3.4×10^{-7}	1.0×10^{-7}
$\Delta\theta$	0.087	0.087

used as input to a third program, FLOCVE, which computed ψ, v_r, v_θ, p, $\tau_{r\theta}$, F_D, and F_L.

Several comments regarding the numerical computations should be noted. First, although the problem was solved in terms of a nondimensional stream function, the angles and distances involved were small and double precision arithmetic was required in all computations. This requirement substantially increased the amount of on-line storage required and was a primary factor in causing the computations to be done in three stages. Second, floating point numbers on the DEC 1099 system must be smaller than 10^{38} and larger than 10^{-38}. This condition was also the source of some difficulty. Third, the size and cost of the programs involved required that the research be limited to a specific case. The parameters for the case considered are summarized in Table 2. Fourth, in Table 1 it is noted that the smallest radial grid size used was 1×10^{-7} m, which was also the radius of the floc particle. Although it would have been desirable to use a smaller radial increment, numerical testing demonstrated that smaller grid spacings had an insignificant effect on the final answer and significantly increased the amount of computer time required. It is noted that r_a is 600 times larger than r_f.

RESULTS

The results of this research are summarized in Figs. 3, 4, and 5. Figure 3 is a small-scale plot of the dimensionless streamlines past the bubble–particle system in the vicinity of $\theta' = 140°$ for two situations: (a) an air bubble with no attached floc particle and (b) an air bubble with a floc particle attached at $\theta' = 140°$. Figure 4 is a large-scale plot of the same region. In these figures it is noted that the region considered is so small that the surface of the air bubble and the streamlines past the air bubble

TABLE 2

Basic Parameter Summary

Parameter	Value	Units
U	7.79×10^{-3}	meters per second
r_a	6×10^{-5}	meters
r_f	1×10^{-7}	meters
μ	1.005×10^{-3}	kilograms per meter second
ρ	998.2	kilograms per cubic meter
$2r_aU\rho/\mu$	0.9	
ν	1.007×10^{-6}	square meters per second
σ	7.36×10^{-2}	newtons per meter
$\rho g^2 r_a 5/\nu^2\sigma$	1×10^{-3}	

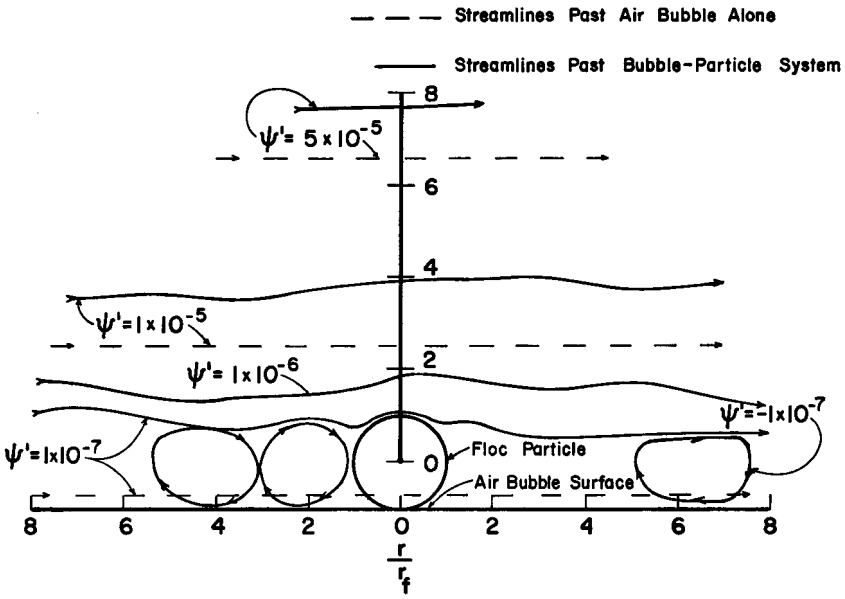

FIG. 3. Dimensionless streamlines past the bubble–particle system for particle attachment at $\theta' = 140°$.

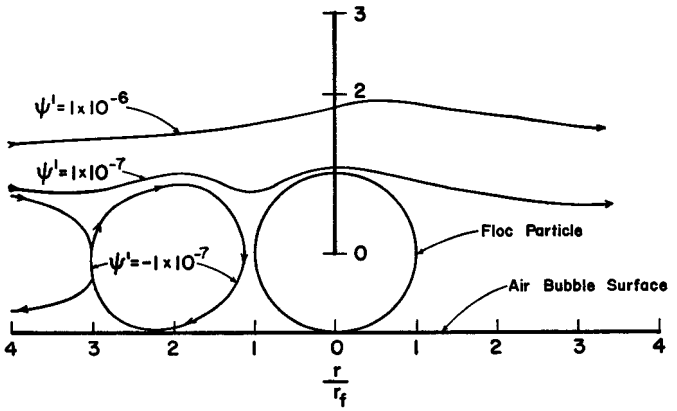

FIG. 4. Dimensionless streamlines past the bubble–particle system for particle attachment at $\theta' = 140°$.

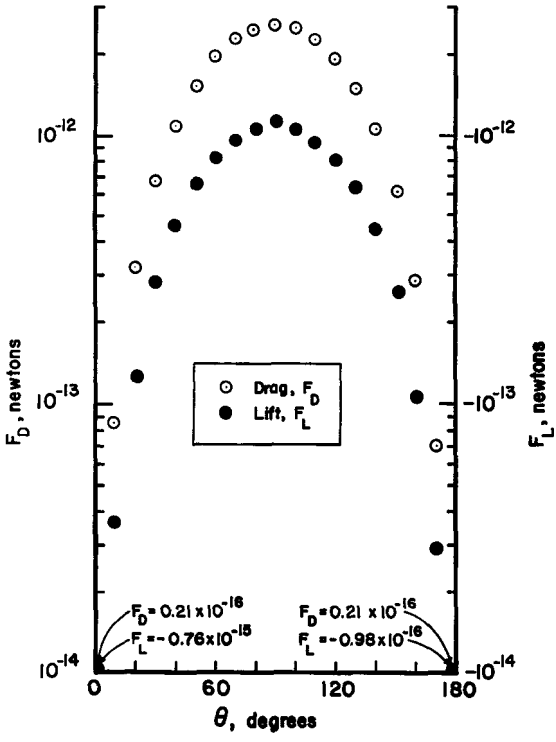

FIG. 5. F_L and F_D as functions of θ' (4.448N = 1 lb).

with no attached floc particle appear as straight lines. The effect of the floc particle is to displace the streamlines outward and distort them, and as the dimensionless distance r/r_f increases, the distortion decreases. In front of the particle there are several closed streamlines which are indicative of the blocking effect of the particle. Behind the particle there is apparently a large region of stagnation. A much finer radial and angular grid would be required to define the streamline patterns in these regions accurately.

In Fig. 5 the drag and lift on the floc particle due to shear and pressure are plotted as functions of θ'. The maximum values of F_D occur at $\theta' = 90$ and 270° while the minima occur at $\theta' = 0$ and 180°. Although finite values of F_D are estimated for attachment at $\theta' = 0$ and 180°, the true value of F_D at these points must be zero since at these points the pressure and shear must be axisymmetric. F_D is a harmonic function of θ'.

With regard to magnitude, the maximum lifts occur at $\theta' = 90$ and 270°,

and the minima at $\theta' = 0$ and 180°. F_L is also a harmonic function of θ'. The surprising conclusion regarding F_L is that the lift is negative in direction; a conclusion which under the assumptions of this research indicates that F_L combines with F_B to bind the floc particle to the air bubble.

The fact that the numerical calculations predict a negative lift is surprising because classical hydrodynamics, e.g., Milne-Thomson (*6*), predicts that as a sphere approaches a plane, which is approximately the situation here, the sphere is repelled from the plane. However, the theoretical and experimental work of Harris (*3*) regarding the approach of a cylindrical body in a viscous shearing flow to a plane at a low Reynolds number demonstrates that the plane attracts the cylinder. Harris (*3*) showed theoretically that this negative lift effect was the result of viscosity in combination with a shearing flow. Thus the case considered here is the extension of Harris' work to a sphere attached to a plane, and the numerical results are consistent with his conclusions.

COMPARISON WITH PREVIOUS WORK

In a previous paper, Currin et al. (*2*) estimated the force tending to separate the floc particle from the rising air bubble by the judicious use of simplifying assumptions. In this work the buoyant force on the rising air bubble was

$$F'_B = \frac{4}{3}\pi r_a^3 \rho g \tag{16}$$

Stokes' law gave the viscous drag on the bubble as

$$F'_D = 6\pi\mu r_a U \tag{17}$$

Combining Eqs. (16) and (17) then yielded an expression for the terminal velocity of rise:

$$U = 2\rho g r_a^2/9\mu \tag{18}$$

The boundary layer thickness of the bubble was estimated as

$$\delta = \pi r_a/3 \tag{19}$$

The drag force on the floc particle was then found by applying Stokes' law to the floc particle where the relative velocity of the fluid in the boundary layer was assumed to be $r_f U/\delta$. The drag force on the floc particle was estimated as

$$F_D = 6\pi r_f \mu \frac{\delta}{r_f U} \tag{20}$$

or

$$F_D = (6.16 \times 10^3) r_a r_f^2 \tag{21}$$

Substitution of the parameters in Table 2 in Eqs. (18), (19), and (21) yields

$$U = 7.79 \times 10^{-3} \text{ m/sec} \tag{22}$$

$$\delta = 6.28 \times 10^{-5} \text{ m} \tag{23}$$

and

$$F_D = 3.69 \times 10^{-14} \text{ N} \tag{24}$$

At this juncture, several comments may be made. First, implicit in the analysis of Currin et al. (*2*) was the assumption that the forces tending to separate the bubble and particle were proportional to the drag force calculated by Eq. (20). The research presented here indicates that, while Eq. (20) provided reasonable estimates of the magnitude of F_L, it completely failed to predict the direction and hence the effect of F_L. Second, from Fig. 5 it is clear that F_L and F_D are not constants but functions of θ'. Third, Wilson (*10*) estimated that F_B was of order 10^{-10} N; hence the binding force is much larger than any of the viscous forces for this flow regime.

APPLICATIONS AND CONCLUSIONS

This research has clearly demonstrated that the interaction of bubbles and floc particles is a very complex problem. In this work, only the very simple case of a single air bubble with a single floc particle pinned to it was considered. This case is, in general, dynamically unstable; the viscous drag on the particle, although very small, would cause the bubble–particle system to rotate. In addition, the assumption that the particle is pinned to the bubble is an extreme idealization. In fact, the nature of the binding force would be such that the particle must be considered free to move about on the bubble surface in response to the forces applied. If this is the case, then the effect of F_B, F_D, and F_L is to roll the floc particle toward $\theta' = 0°$. Although the detailed analysis of this movement would be interesting, it would obscure the fact that as the air bubble moves up through the column, it randomly encounters many particles, and it is the latter problem which must be solved.

On the basis of the research presented here, it is asserted that the design of an optimum air bubble for foam flotation, i.e., a bubble which is large enough to encounter and collect many particles but small enough so that the particles are not stripped from the bubble, is composed of two problem areas which can be considered separately. The first problem area

concerns the time previous to initial bubble–particle contact. In this area the particle can initially be viewed as a point mass traveling on a streamline subject to F_B, a centrifugal force due to streamline curvature, and the net resultant of the buoyant and gravitational forces. As the particle moves closer to the bubble, a fourth force becomes important: the viscous force termed F_L in this research. For small Reynolds numbers, F_L is negative and the bubble attracts the particle. At high Reynolds numbers, F_L may be positive and the bubble would repel the particle. The work of Harris (*3*) is not sufficient to establish the limiting value of Re.

The second problem area occurs after contact between the bubble and the particle is established. F_B, F_D, and F_L act to roll the particle back on the bubble toward $\theta' = 0°$, and after a series of random bubble–particle collisions an axisymmetric cap of floc particles would be formed on the bubble in the vicinity of $\theta' = 0°$, Fig. 6. Thus the second problem area concerns the fluid motion past the bubble with a particle cap. This flow can be computed from Eqs. (1) and (2) for Re < 1 or from the Prandtl boundary layer equations (*7*) for Re > 1. The cap fails when the pressure, shear, and gravitational forces on the cap combine to "pop" a particle out of the cap and off the bubble.

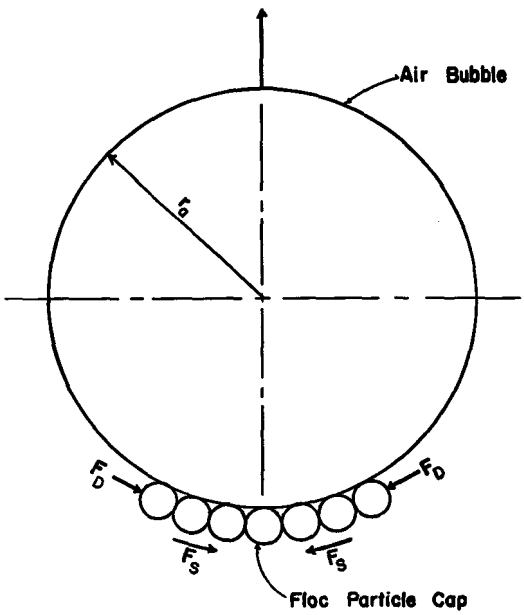

FIG. 6. Schematic of air bubble with a cap of floc particles at $\theta' = 0°$.

It must be noted that the numerical results of this research should be treated as order of magnitude estimates of the viscous forces involved rather than as exact answers. The assumptions required to obtain these results were extreme idealizations of the true situation. However, these estimates have led to the formulation of two new models which are much more tractable and lend themselves, in the numerical sense, to exact solution. It is hoped that this research will be of general use in guiding other investigators in exploring the field of foam flotation.

SYMBOLS

F_L	lift force
F_D	drag force
F'_D	drag on air bubble
F_B	binding force
F'_B	buoyant force
g	gravitational acceleration
p	pressure
r_a	radius of air bubble
r_f	radius of floc particle
r, θ	polar coordinate system centered at the center of the floc particle
r', θ'	polar coordinate system centered at center of the air bubble
U	free stream velocity
v_n	velocity normal to boundary
v_t	velocity tangent to boundary
v_r	radial velocity
v_θ	theta velocity
$\mathbf{v}$	velocity vector
δ	boundary layer thickness
μ	absolute viscosity
ν	kinematic viscosity
ρ	fluid density; shear stress acting in the θ direction on a plane whose normal is the y direction
σ	liquid surface tension parameter
ψ	Stokes stream function
ψ'	dimensionless stream function

NUMERICAL COEFFICIENTS

$$\alpha_0 = 4 \sin^3 \theta \left(\frac{\Delta r}{r^3} - \frac{\Delta \theta^2}{\Delta r^2} - \frac{1}{r^2} \right)$$

$$\alpha_1 = 2\sin^3\theta\left(\frac{3\Delta\theta^2}{\Delta r^2} + \frac{4}{r^2} + \frac{3\Delta r^2}{r^4\Delta\theta^2} - \frac{6\Delta r^2}{r^4}\right) - \frac{2\Delta r^2}{r^4}(\cos^2\theta\sin\theta + 2\sin\theta)$$

$$\alpha_2 = \frac{\Delta\theta^2\sin^3\theta}{\Delta r^2}$$

$$\alpha_3 = -4\sin^3\theta\left(\frac{\Delta\theta^2}{\Delta r^2} + \frac{\Delta r}{r^3} + \frac{1}{r^2}\right)$$

$$\alpha_4 = \frac{\Delta\theta^2\sin^3\theta}{\Delta r^2}$$

$$\alpha_5 = \cos\theta\left(\frac{2\Delta\theta\sin^2\theta}{r^2} + \frac{\Delta r^2\cos\theta\sin\theta}{r^4} + \frac{2\Delta r^2\sin^2\theta}{\Delta\theta r^4}\right) - \left(\frac{3\Delta r^2\,\Delta\theta\sin^2\theta}{r^4} - \frac{3\Delta r^2\Delta\theta}{2r^4}\right) + 2\sin^3\theta\left(\frac{3\Delta r^2}{r^4} - \frac{2}{r^2} - \frac{2\Delta r^2}{\Delta\theta^2 r^4}\right) + \frac{2\Delta r^2\sin\theta}{r^4}$$

$$\alpha_6 = \frac{\Delta r^2\sin^3\theta}{r^4\Delta\theta^2} - \frac{\Delta r^2\cos\theta\sin^2\theta}{\Delta\theta r^4}$$

$$\alpha_7 = \cos\theta\left(\frac{3\Delta\theta\Delta r^2\sin^2\theta}{r^4} + \frac{3\Delta\theta\Delta r^2}{2r^4} - \frac{2\Delta\theta\sin^2\theta}{r^2} + \frac{\Delta r^2\cos\theta\sin\theta}{r^4} - \frac{2\Delta r^2\sin^2\theta}{\Delta\theta r^4}\right) + 2\sin^3\theta\left(\frac{3\Delta r^2}{r^4} - \frac{2}{r^2} - \frac{2\Delta r^2}{r^4\Delta\theta^2}\right) + \frac{2\Delta r^2\sin\theta}{r^4}$$

$$\alpha_8 = \frac{\Delta r^2}{r^4}\left(\frac{\cos\theta\sin^2\theta}{\Delta\theta} + \frac{\sin^3\theta}{\Delta\theta^2}\right)$$

$$\alpha_9 = \cos\theta\sin^2\theta\left(\frac{\Delta r\Delta\theta}{r^3} - \frac{\Delta\theta}{r^2}\right) + 2\sin^3\theta\left(\frac{1}{r^2} - \frac{\Delta r}{r^3}\right)$$

$$\alpha_{10} = \cos\theta\sin^2\theta\left(\frac{\Delta\theta}{r^2} - \frac{\Delta r\Delta\theta}{r^3}\right) + 2\sin^3\theta\left(\frac{1}{r^2} - \frac{\Delta r}{r^3}\right)$$

$$\alpha_{11} = -\cos\theta \sin^2\theta\left(\frac{\Delta r\Delta\theta}{r^3} + \frac{\Delta\theta}{r^2}\right) + 2\sin^3\theta\left(\frac{\Delta r}{r^3} + \frac{1}{r^2}\right)$$

$$\alpha_{12} = \cos\theta \sin^2\theta\left(\frac{\Delta r\Delta\theta}{r^3} + \frac{\Delta\theta}{r^2}\right) + 2\sin^3\theta\left(\frac{\Delta r}{r^3} + \frac{1}{r^2}\right)$$

REFERENCES

1. G. K. Batchelor, *An Introduction to Fluid Dynamics*, Cambridge University Press, Cambridge, England, 1970, pp. 367–370.
2. B. L. Currin, F. J. Potter, D. J. Wilson, and R. H. French, *Sep. Sci. Technol.*, *13*, 285 (1978).
3. S. D. Harris, Jr., "Experimental Determination of the Velocity Gradient in Two-Dimensional Turbulent Flow," M.S. Thesis, Vanderbilt University, 1966.
4. H. Lamb, *Hydrodynamics*, 6th ed., Dover, New York, 1945.
5. R. Lemlich (ed.), *Adsorption Bubble Separation Techniques*, Academic, New York, 1972.
6. L. M. Milne-Thomson, *Theoretical Hydrodynamics*, Macmillan, New York, 1969.
7. H. Schlichting, *Boundary Layer Theory*, 2nd ed., McGraw-Hill, New York, 1960.
8. R. L. Street, *Analysis and Solution of Partial Differential Equations*, Brooks Cole, Monterrey, California, 1973.
9. F. M. White, *Viscous Fluid Flow*, McGraw-Hill, New York, 1974, pp. 200–215.
10. D. J. Wilson, *Sep. Sci. Technol.*, *13*, 107 (1978).

Received by editor November 5, 1979